

Beta Decay of  $^{17}\text{N}^\dagger$ 

A. R. Poletti and J. G. Pronko

*Lockheed Palo Alto Research Laboratory, Palo Alto, California 94304*

(Received 24 May 1973)

The delayed-neutron and  $\gamma$ -ray spectra following the  $\beta$  decay of  $^{17}\text{N}$  have been investigated using the  $\beta$ - $n$  time-of-flight method,  $\beta$ - $\gamma$  coincidences, and neutron spectrometry. The following branchings have been determined for the  $\beta$  decay of  $^{17}\text{N}$  to established energy levels in  $^{17}\text{O}$ : decay to ground state ( $1.7 \pm 0.5\%$ ), 0.87 MeV ( $2.9 \pm 0.5\%$ ), 3.06 MeV ( $0.54 \pm 0.08\%$ ), 4.55 MeV ( $37.9 \pm 1.8\%$ ), 5.377 MeV ( $51.1 \pm 1.5\%$ ), and 5.935 MeV ( $5.8 \pm 0.6\%$ ). The latter three states are particle unstable and decay by the emission of neutrons to the ground state of  $^{16}\text{O}$ . The energies of these neutron groups as determined by us were, respectively,  $0.385 \pm 0.004$ ,  $1.163 \pm 0.014$ , and  $1.675 \pm 0.024$  MeV. The results are discussed and compared to theoretical calculations. The measured  $\beta$ -decay strengths are compared to the strengths of corresponding transitions in the  $\beta$  decay of the mirror nucleus  $^{17}\text{Ne}$ .

## I. INTRODUCTION

Of all the nuclei which can be reached by two-neutron transfer on stable nuclides there are just four which can possibly give  $\beta$ -delayed neutrons. These are  $^9\text{Li}$ ,  $^{13}\text{B}$ ,  $^{16}\text{C}$ , and  $^{17}\text{N}$ . The neutron spectroscopy of  $^9\text{Li}$  has been investigated by Macefield, Wakefield, and Wilkinson,<sup>1</sup> and of  $^{13}\text{B}$  by Jones, Harris, McEllistrem, and Alburger.<sup>2</sup> Except for the fact that  $^{16}\text{C}$  does give rise to delayed neutrons,<sup>3</sup> no further evidence concerning their origin is available. The observation of delayed neutrons following the  $\beta$  decay of  $^{17}\text{N}$  has been reported by a number of groups. The ( $4.14 \pm 0.04$ )-sec neutron activity discovered by Knable *et al.*<sup>4</sup> was shown by Alvarez<sup>5</sup> to be due to the emission of neutrons following the  $\beta$  decay of  $^{17}\text{N}$ . Alvarez<sup>5</sup> demonstrated, by direct observation of  $\beta$ -neutron coincidences, the correctness of the Bohr-Wheeler<sup>6</sup> hypothesis that the delayed neutrons observed, for instance, following fission were from extremely short-lived states populated by  $\beta$  decay. These states were unstable against the emission of a neutron, and the observed lifetime of the neutron "activity" was thus the lifetime of the parent nucleus.

The measurements of the energy spectrum of the neutrons by Alvarez,<sup>5</sup> Hayward,<sup>7</sup> and Perlow *et al.*<sup>8</sup> were hampered by lack of resolution; however, Hayward,<sup>7</sup> in one possible interpretation of her results, suggested the possibility of two neutron groups at approximately 1 MeV and "nearer 1.8 MeV." Perlow *et al.*<sup>8</sup> observed two groups and gave their energies as ( $1.22 \pm 0.06$ ) and ( $0.426 \pm 0.018$ ) MeV. They also observed that the ratio of the intensity of the high-energy group to the low-energy group was 1.6. An abstract by Gilat, O'Kelley, and Eichler<sup>9</sup> reported three neutron groups with energies of ( $1807 \pm 40$ ), ( $1213 \pm 20$ ), and ( $404 \pm 10$ ) keV. The relative intensities found

by these workers were quoted with no assigned errors by Silbert and Hopkins,<sup>10</sup> who made a comprehensive study of the decay of  $^{17}\text{N}$  to bound states in  $^{17}\text{O}$ . The half-life of  $^{17}\text{N}$  has been reported by several workers.<sup>11,12</sup> The mean value of the four earlier measurements is ( $4.16 \pm 0.01$ ) sec. The most recent measurement by Alburger and Wilkinson<sup>12</sup> gives  $4.169 \pm 0.008$  sec. It is in excellent agreement with the mean of the earlier determinations and for the purposes of further discussion we adopt the value  $4.165 \pm 0.007$  sec as the half-life of  $^{17}\text{N}$ .

Quite apart from the intrinsic interest of investigating the  $\beta$  decay of a nucleus which gives rise to delayed neutrons, there were three main reasons for undertaking this work. The first arises from the current interest<sup>13</sup> in the question of the extent to which mirror symmetry is obeyed in the  $\beta$  decay of mirror pairs. The second arises from the work of Towner, Warburton, and Garvey<sup>14</sup> on the strengths of the unique  $n$ -forbidden  $\beta$  decays. Finally, the measured  $\beta$ -decay strengths provide a touchstone for testing the predictions of models which seek to describe the structure of mass-17 nuclei.<sup>15</sup>

## II. EXPERIMENTAL PROCEDURE

A. Production of  $^{17}\text{N}$ 

The  $^{17}\text{N}$  activity was produced by tritium bombardment of  $^{15}\text{N}_2$  gas, contained at a pressure of approximately 1 atm, in a cylindrical glass target cell of length 7.0 cm and wall thickness 1.2 mm. The enrichments used were between 95 and 99%  $^{15}\text{N}$ . The 2.9-MeV triton beam, provided by the Lockheed 3-MV Van de Graaff accelerator, entered the target cell through a 0.025-mm-thick nickel window. The beam was chopped by a solenoidally actuated tantalum beam stop which was located 5 m

before the target. The solenoid,<sup>16</sup> operated by direct current, was controlled by a programmer<sup>16</sup> which in addition provided a logic output that was used to control the acquisition of data. The length of the total irradiate-count cycle as well as the "count" and "irradiate" phases could be set by digiswitches. In addition, a time delay between the "irradiate" and "count" phases of the cycle ensured that sufficient time had elapsed for the beam chopper to be completely closed before counting began. Count and irradiate times were set approximately equal and were each 4 sec.

### B. Scintillation and Time-of-Flight Spectroscopy

In order to establish the intensities of the  $\beta$  decay to neutron-emitting levels in  $^{17}\text{O}$  with respect to the decay to  $\gamma$ -emitting levels, it was necessary to observe the  $\gamma$ -ray spectrum in coincidence with the  $\beta$  particles and, at the same time, to observe the spectrum of the neutrons resulting from the  $\beta$  decay of  $^{17}\text{N}$ . The neutron spectrum was observed by using a time-of-flight (TOF) method. The disposition of the three detectors involved as well as the target cell is sketched in Fig. 1. The  $\beta$  detector, consisting of a cylinder of NE102 5 cm thick and 7.5 cm in diameter optically coupled via a small conical light guide to an RCA 8575 photomultiplier, was positioned vertically above the glass target cell with its front face 1.5 cm above the center of the cell. The  $\gamma$ -ray detector was a 15.2-cm-thick by 12.7-cm-diam NaI(Tl) crystal optically coupled to an RCA 8055 photomultiplier. It was shielded from the  $\beta$  activity by 1.14 cm of carbon and 0.45 cm of copper. This detector was

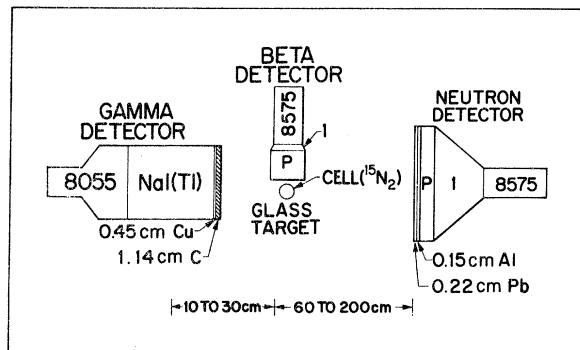


FIG. 1. A sketch showing the disposition of the detectors used in the  $\beta$ - $n$  time-of-flight and  $\beta$ - $\gamma$  coincidence experiment. The beam was into the paper. A small gas-handling system enable the target cell to be filled with  $^{15}\text{N}_2$  (or in the efficiency calibrations, with  $\text{CF}_4$ , Ne, or  $^{14}\text{N}_2$ ). The letter  $P$  and the number 1 signify, respectively, NE102 plastic scintillators and lucite light guides.

set in a horizontal plane containing the target cell. The distance from the front face of the detector to the center of the target cell was varied (in different runs) between 11.8 and 30.0 cm. To detect the neutrons a disc of NE102, 2.5 cm thick by 20.4 cm in diameter, was optically coupled via a conical light guide to an RCA 8575 photomultiplier. The scintillator was shielded from the target by 0.22 cm of lead and 0.15 cm of aluminum. This detector was set at distances ranging from 60 to 200 cm from the center of the target during the course of the experiment.

A block diagram of the electronic apparatus used to acquire the  $\beta$ - $n$  time-of-flight spectrum and the simultaneous  $\gamma$ -ray spectrum is shown in Fig. 2. Fast timing pulses were derived from the anodes of the photomultipliers viewing the  $\beta$  and neutron scintillators. The pulse from the  $\beta$  detector (delayed by 500 nsec) was used to drive the stop channel of a time-amplitude converter (TAC). The start signal was obtained from the neutron detector in overlap coincidence with a 500-nsec-wide pulse derived from the  $\beta$ -detector fast pulse. (In this way the start channel was driven only at a rate equal to that provided by the output of a slow

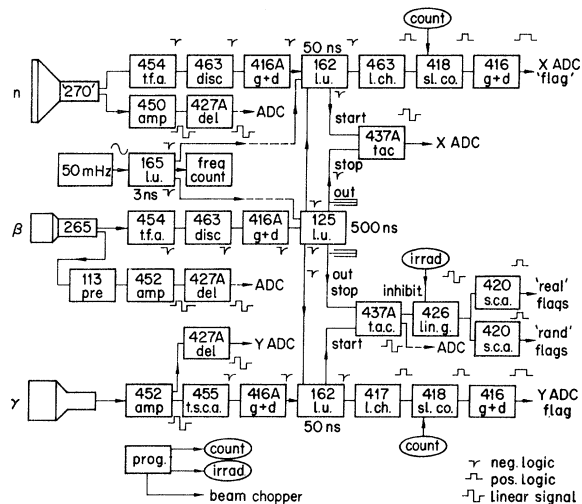


FIG. 2. A diagram to illustrate the arrangement and interconnection of the electronic modules used in the  $\beta$ - $n$  time-of-flight and  $\beta$ - $\gamma$  coincidence experiment. Except for the programmer the modules are commercially available. The signals at different points in the system are indicated. The voltage levels provided by the programmer are indicated by the encircled words "count" and "irrad." The abbreviations used on the diagram are as follows: amp, amplifier; del, delay amplifier; disc, discriminator;  $g+d$ , gate and delay; l. ch., logic-level changer; lin. g., linear gate; l. u., logic unit; pre, preamplifier; prog., programmer; s.c.a., single-channel analyzer; sl. co., slow coincidence; t.a.c., time-to-amplitude converter; t.f.a., timing filter amplifier.

coincidence circuit of 500-nsec resolving time.) The TAC was connected to one of two analog-digital converters (X ADC) interfaced to an SEL 810A general-purpose digital computer. The ADC was flagged only during the "count" period by demanding a "coincidence" between the "count" level from the programmer and the logic pulse signifying a slow  $n$ - $\beta$  coincidence. A neutron- $\beta$  time-of-flight spectrum obtained with a similar arrangement to that described above is shown in Fig. 3. The time calibration was obtained directly in terms of a frequency by using a 50-mHz crystal-controlled oscillator to drive a Lecroy model-165 logic-unit set to deliver 3-nsec-wide pulses. These 50-mHz pulses were fanned out to either side of the TAC (see Fig. 2) by connecting the outputs of the 165 to the input of the Lecroy 162 and 125 logic units and increasing the coincidence-level requirement, respectively, from 2 to 3 and from 1 to 2. Separate  $\gamma$ -ray sources placed near each detector (and shielded from the other) provided the random coincidences which (modulated by the 50-mHz signal) gave the calibration spectrum displayed in the lower part of the figure. A measurement of the frequency then gave the time calibration with more than sufficient accuracy.

The arrangement of the electronics used to obtain the  $\beta$ - $\gamma$  coincidences was similar to that used

to obtain the  $\beta$ - $n$  time-of-flight spectrum and is shown in the lower part of Fig. 2. In this case it was the output of the  $\gamma$  linear signal which was fed to a second ADC (Y ADC) interfaced to the same computer. The output of the TAC was fed through a linear gate to two single-channel analyzers which were set, respectively, on the coincidence peak ("real" flags) and on the random background ("random" flags). These flags were accepted by the computer as part of the specification of a  $\beta$ - $\gamma$  coincidence event. The linear gate was inhibited during the "irradiate" part of each cycle. Figure 4 presents both the  $\beta$ - $n$  time-of-flight spectrum and the simultaneously acquired ( $\beta$ - $\gamma$ )  $\gamma$ -ray spectrum obtained with the setup sketched in Fig. 2. The simultaneous acquisition of both the neutron and  $\gamma$ -ray spectra minimized dead-time problems: Except for the slight differences in the counting rates in the neutron and  $\gamma$ -ray detectors, dead-time losses were the same for both spectra. The relative branchings to both neutron and  $\gamma$ -emitting levels were thus directly obtainable (once the detector efficiencies were known) from the areas of the various peaks.

### C. Determination of Detector Efficiencies

To obtain the percentage branching it was necessary to determine the relative efficiency of the  $\beta$

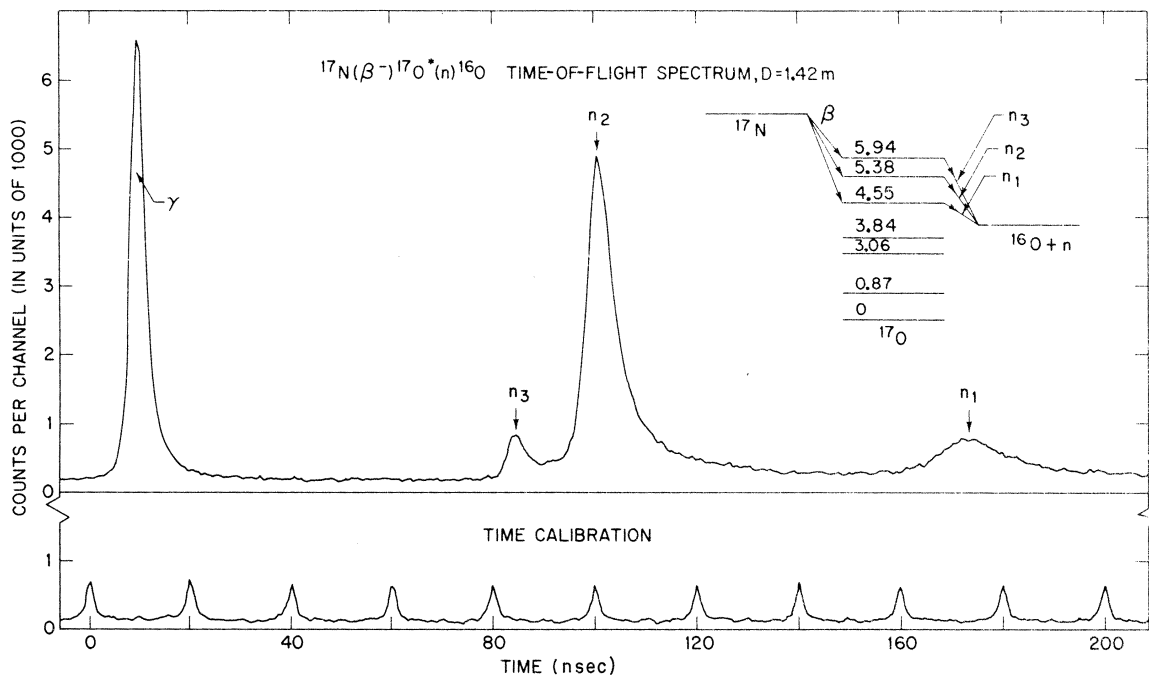


FIG. 3. Neutron- $\beta$  time-of-flight spectrum observed following the  $\beta$  decay of  $^{17}\text{N}$ . The flight path was 1.42 m. The peak marked  $\gamma$  is due to real  $\beta$ - $\gamma$  coincidences arising from the decay of  $^{17}\text{N}$  to  $\gamma$ -emitting levels in  $^{17}\text{O}$  and from the  $\beta$  decay of  $^{16}\text{N}$ . The peaks marked  $n_1$ ,  $n_2$ , and  $n_3$  are due to the delayed-neutron groups depopulating the levels at 4.55, 5.38, and 5.94 in  $^{17}\text{O}$ . Their energies are, respectively, 0.387, 1.162, and 1.687 MeV. In the lower part of the figure the time-calibration spectrum is shown. The method used to obtain this calibration is described in the text.



D.  $^3\text{He}$ -Proportional-Counter Measurements

In the  $\beta$ - $n$  TOF experiment, because of the extremely low light output for low-energy neutrons<sup>21</sup> it was not possible to set the discriminator low enough (yet still above the noise) so that a significant fraction of the proton recoils associated with the lowest-energy neutron group ( $E_n = 0.387$  MeV) were recorded. Consequently, the detection efficiency calculated for this group could not be relied upon. Even a direct measurement of this efficiency was difficult and of limited accuracy.

TABLE I. Detector efficiencies used in extracting relative decay branchings.

Radiation	Energy (MeV)	Efficiency
$\beta^a$	8.68	0.200
	7.81	0.200
	5.62	0.200
	4.13	0.178
	3.30	0.138
	2.74	0.113
$\gamma^b$	0.87 <sup>c</sup>	$(3.78 \pm 0.07) \times 10^{-3}$
	2.19 <sup>c</sup>	$(2.45 \pm 0.05) \times 10^{-3}$
	0.87 <sup>d</sup>	$(5.05 \pm 0.10) \times 10^{-3}$
	2.19 <sup>d</sup>	$(3.18 \pm 0.06) \times 10^{-3}$
$n^e$	0.39	f
	1.16	$0.28 \pm 0.03$
	1.69	$0.26 \pm 0.03$
$n^g$	0.39	0.72
	1.16	0.62
	1.69	0.51

<sup>a</sup> For the  $\beta$  detector, the efficiencies listed are absolute. They were measured with a discriminator setting of 70 keV. Only the relative uncertainties are of importance in this experiment. These were taken to be  $\pm 2\%$ . There was 409 mg/cm<sup>2</sup> of material between the target and the detector.

<sup>b</sup> Absolute peak efficiencies measured at the specified target-to-detector distances with the carbon and copper shielding in place in front of the detector.

<sup>c</sup> Target center to detector front face ( $d$ ) equals 30 cm.

<sup>d</sup>  $d = 25$  cm.

<sup>e</sup> Plastic scintillation detector. The relative efficiencies quoted were calculated for a discriminator setting equivalent to a 200-keV neutron energy, as explained in the text. The quoted efficiencies are corrected for attenuation of the neutron beam by material between the target and detector. The solid angles subtended by the detector at distances of 100 and 160 cm from the target were taken as  $2.54 \times 10^{-3}$  and  $1.00 \times 10^{-3}$ , respectively.

<sup>f</sup> Efficiency calculation unreliable at this energy.

<sup>g</sup>  $^3\text{He}$  proportional counter. Relative efficiencies were calculated as described in the text. The uncertainty in the efficiency for detection of the low-energy group with respect to the efficiency for detection of the 1.16-MeV group was estimated as  $\pm 5\%$ . For the high-energy group, the comparable quantity was  $\pm 10\%$ .

In view of this we undertook a further measurement using a high-pressure  $^3\text{He}$  proportional counter.

The use of  $^3\text{He}$  proportional counters in neutron spectrometry has been described by Batchelor and Morrison.<sup>22</sup> The detector depends on the exothermic reaction  $^3\text{He}(n, p)^3\text{H}$ ,  $Q = +0.765$  MeV. Unlike recoil detectors (e.g. plastic scintillators) a monoenergetic neutron group thus gives rise to a peak in the pulse-height spectrum and not a continuous distribution. Under these circumstances, the relative efficiency of the detector as a function of energy can be calculated with a reasonable degree of confidence from the published<sup>23</sup>  $^3\text{He}(n, p)^3\text{H}$  cross sections. Corrections need to be made for the differing attenuations<sup>23</sup> of the neutron groups in the walls of the detector (and also the glass wall of the target chamber). In addition, since the ranges of the tritons and protons produced in the detector are not insignificant with respect to its width, a correction must be made for "wall effects"; these arise because some of the events will take place near the walls and either the proton or triton (or both) will hit the wall before coming to rest, thus removing a count from the full-energy peak. Another disadvantage of the detector is its very low efficiency for detecting fast neutrons. It is, however, a very sensitive detector for thermal neutrons ( $\sigma_{\text{th}} = 5330$  b). To reduce the effect of this peak, the detector was covered with a sheet of

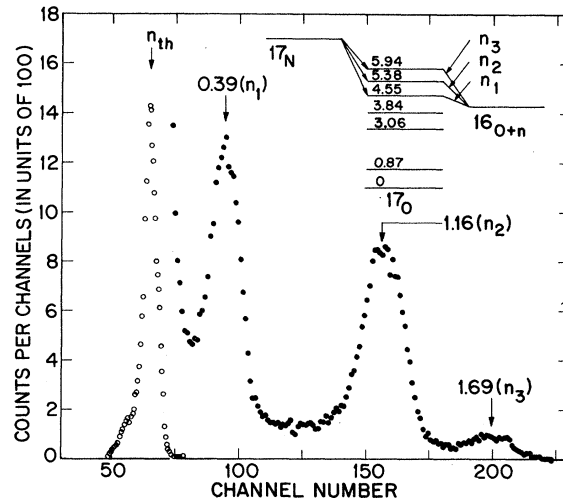


FIG. 5. The delayed-neutron spectrum observed following the  $\beta$  decay of  $^{17}\text{N}$ . The detector was a  $^3\text{He}$  proportional counter. The three neutron groups arising from the decay are clearly seen. The small inset gives the response to thermal neutrons. The relative areas of the peaks due to the fast neutron groups (when corrected for relative detector efficiency) give the relative intensities for the  $\beta$  decay of  $^{17}\text{N}$  to neutron unstable levels in  $^{17}\text{O}$ .

cadmium 0.025 cm thick.

The detector which we used was 2.5 cm in diameter and had a sensitive length of 30.5 cm. It was filled to a pressure of 2.3 atm with  $^3\text{He}$  and 4.7 atm with krypton. An addition of 2.5%  $\text{CO}_2$  was used as a quench gas. The correction for wall effects was made using the method and results of Batchelor, Aves, and Skyrme.<sup>24</sup> Figure 5 shows the spectrum obtained when the detector was placed beside the glass target cell and exposed to the delayed neutrons following the  $\beta$  decay of  $^{17}\text{N}$ . With air in the target cell (instead of  $^{15}\text{N}_2$ ) the background above channel 80 was smooth and because of the low count rate was negligible compared to the spectrum accumulated with  $^{15}\text{N}_2$  in the cell. The resolution of the detector was 9.1% for the thermal peak. A much better resolution can be obtained with lower filling pressures, but wall effects would be much more serious. The three delayed neutron groups following the  $\beta$  decay of  $^{17}\text{N}$  are clearly seen in the figure.

### III. RESULTS

#### A. Neutron Energy Measurements

The mean energies of the three neutron groups, shown for instance in Fig. 3, were determined directly from flight-time differences for changes in the scintillation neutron detector-target distance of 60, 80, and 120 cm in different runs. The method used to calibrate the TAC was described in Sec. II B. We obtained mean energies of  $0.385 \pm 0.004$ ,  $1.163 \pm 0.014$ , and  $1.675 \pm 0.024$  MeV for the three neutron groups observed. These energies correspond to level energies of  $4.552 \pm 0.004$ ,  $5.378 \pm 0.014$ , and  $5.921 \pm 0.026$  MeV in  $^{17}\text{O}$ . We can therefore identify them unambiguously with established<sup>11</sup> levels at  $4.554 \pm 0.006$  MeV ( $J^\pi = \frac{3}{2}^-$ ),  $5.377 \pm 0.003$  MeV ( $J^\pi = \frac{3}{2}^-$ ), and  $5.935 \pm 0.003$  MeV ( $J^\pi = \frac{1}{2}^-$ ) in  $^{17}\text{O}$ .

#### B. $\beta$ -Decay Branching Measurements

The primary data consisted of a number of interconnecting and sometimes overlapping peak area ratios. These, when corrected for detector effi-

ciencies and (if necessary) attenuation, yielded a set of intensity ratios (the primary data). A suitable combination and normalization of this primary data gave the relative decay intensities which in turn, when combined with the measured half-life of  $^{17}\text{N}$ , yielded the partial half-lives of the various decay modes and thence the  $ft$  values. The various sources of the primary data were:

- (i) the coincidence  $\gamma$ -ray spectrum,
- (ii) the TOF neutron spectrum,
- (iii) the simultaneously acquired coincidence  $\gamma$ -ray spectrum and neutron TOF spectrum,
- (iv) the  $^3\text{He}$ -proportional-counter neutron spectrum, and
- (v) the singles  $\beta$  spectrum.<sup>10</sup>

Table II summarizes the primary data. The first column specifies the two radiations of interest, the second column gives the value obtained for the ratio of the intensities of the two radiations, while the third column gives in an abbreviated form the source of the measurement. In the present experiment we did not measure the ratio of the intensities for decay to the first excited and ground states because of background problems. Instead we take the value quoted by Silbert and Hopkins.<sup>10</sup> The rest of the intensity ratios listed in Table II are from the present experiment. In Table III we list the percentage branchings for the  $\beta$  decay of  $^{17}\text{N}$  which we have derived from the data of Table II. The values for the decay to the 0.87- and 3.06-MeV levels agree very nicely with those found in Ref. 10. Two further comparisons can be made: Silbert and Hopkins<sup>10</sup> obtain  $6.8 \pm 0.9$  for the relative intensities of the 0.87- and 2.19-MeV  $\gamma$  rays. We obtain  $6.36 \pm 0.20$ . Although the results are not completely independent, the percentage of all decays to bound states in  $^{17}\text{O}$  are also in excellent agreement. We obtain  $(5.14 \pm 0.72)\%$  while Silbert

TABLE III.  $\beta$  decay of  $^{17}\text{N}$ . The first column specifies the decay by listing the excitation (in MeV) of the level in  $^{17}\text{O}$  to which the decay proceeds. The second column (derived from Table II) gives the decay intensity as a ratio of the decay intensity to the 5.38-MeV level. The third column displays the derived percentage branchings. These values are compared with the results quoted by Silbert and Hopkins in the last column.

TABLE II. Intensity ratios observed in the  $\beta$  decay of  $^{17}\text{N}$ .

Ratio	Value	Source
$I(E_\beta = 7.81)/I(E_\beta = 8.68)$	$1.7 \pm 0.4$	Ref. 10
$I(E_\gamma = 0.87)/I(E_n = 1.16)$	$0.0667 \pm 0.0095$	TOF + NaI(Tl)
$I(E_\gamma = 2.19)/I(E_n = 1.16)$	$0.0105 \pm 0.0015$	TOF + NaI(Tl)
$I(E_n = 0.39)/I(E_n = 1.16)$	$0.742 \pm 0.054$	$^3\text{He}$ proportional counter
$I(E_n = 1.69)/I(E_n = 1.16)$	$0.126 \pm 0.018$	$^3\text{He}$ proportional counter
$I(E_n = 1.69)/I(E_n = 1.16)$	$0.103 \pm 0.018$	TOF

Decay to	Ratio	Branch (%)	
		Present	Ref. 10
0	$0.0331 \pm 0.0095$	$1.7 \pm 0.5$	$1.6 \pm 0.5$
0.87	$0.0562 \pm 0.0095$	$2.9 \pm 0.5$	$2.6 \pm 0.5$
3.06	$0.0105 \pm 0.0015$	$0.54 \pm 0.08$	$0.46 \pm 0.11$
4.55	$0.742 \pm 0.054$	$37.9 \pm 1.8$	(45)
5.38	(1.0)	$51.1 \pm 1.5$	(45)
5.94	$0.114 \pm 0.012$	$5.8 \pm 0.6$	(5)

and Hopkins<sup>10</sup> quote  $(4.66 \pm 0.75)\%$ . Finally, although the results must have been regarded as preliminary, the branchings quoted by Silbert and Hopkins<sup>10</sup> for decay to the neutron emitting levels are not in unreasonable agreement with those which we have determined. For the purposes of further discussion we will use the branchings determined in the present work, since no errors were quoted in Ref. 10.

In Table IV we show the  $ft$  values for six observed  $\beta$ -decay transitions from  $^{17}\text{N}$  and compare them with the mirror transitions<sup>25</sup> from  $^{17}\text{Ne}$  as well as with theoretical calculations.<sup>15</sup> The first column specifies the spin and parity of the final state involved while the second and fourth columns specify their energies in  $^{17}\text{O}$  and  $^{17}\text{F}$ , respectively. The allowed  $ft$  values ( $f_0t$ ) for the odd-parity states were calculated using the Fermi function as defined, for instance, in Konopinski.<sup>28</sup> A screening correction<sup>29</sup> was made, but no radiative correction. The first forbidden  $ft$  value ( $f_1t$ ) for the decay to the ground state includes a correction for the finite de Broglie wavelength of the electron<sup>30</sup> and for screening, but again no radiative correction was made. For comparison an  $f_1t$  value calculated in the same way is also shown for the decay to the first excited state. We will discuss the results summarized in this table in the following section.

#### IV. DISCUSSION

##### A. Comparison with Theoretical Calculations

The allowed  $\beta$  decay of the  $T = \frac{3}{2}$ , mass-17 nuclei has been investigated by Margolis and de Takacsy<sup>15</sup> and by Hirata.<sup>15</sup> Margolis and de Takacsy carried out their calculations assuming a two-particle-one-hole structure (2p-1h) for the levels of interest. They found that the binding of the lowest  $\frac{1}{2}^-$ ,  $T = \frac{1}{2}$  state in  $^{17}\text{O}$  was too weak by about 1.5 MeV. This can be interpreted as an indication of the effect of neglecting the 4p-3h components of the wave functions. Hirata<sup>15</sup> considered both 2p-1h and 4p-3h contributions and used a somewhat restricted basis. He concluded that while the 2p-1h con-

figuration was the major component for two lowest-lying  $\frac{1}{2}^-$  states and two lowest-lying  $\frac{3}{2}^-$  states, the intensity of the 4p-3h configuration varied from 5% for the lowest-lying  $\frac{1}{2}^-$  state to 19% for the second  $\frac{1}{2}^-$  state. Ellis and Engeland<sup>15</sup> in their weak-coupling calculations also showed that an improved description of the states of interest could be obtained by including the 4p-3h configuration. They concluded, however, that the 4p-3h configuration was a much more important component of the wave functions: The intensity of the 4p-3h component in the  $T = \frac{1}{2}$  states of interest ranged from 34% for the lowest  $\frac{1}{2}^-$  state to 61% for the second  $\frac{1}{2}^-$  state.

In the second to last column of Table IV we list the  $f_0t$  values calculated by Hirata.<sup>15</sup> Somewhat similar values were also obtained by Margolis and de Takacsy.<sup>15</sup> Neither calculation explains the strength of the transition to the second  $\frac{3}{2}^-$  state (at 5.38 MeV in  $^{17}\text{O}$ ). Hirata's calculation<sup>15</sup> gives values closer to the experimental ones for the other two strong transitions while both calculations are in qualitative agreement with the experimental  $f_0t$  value for the weak transition to the first  $\frac{1}{2}^-$  state (at 3.06 MeV in  $^{17}\text{O}$ ).

At first glance the  $f_0t$  value for decay to the first  $\frac{1}{2}^-$  state at 3.06 MeV should be much smaller than the experimentally observed value of  $7.56 \times 10^6$ . An explanation for the hindrance of this transition was first given by Margolis and de Takacsy<sup>15</sup> in terms of destructive interference between the intrinsically strong  $\beta$ -decay matrix elements connecting the  $^{17}\text{N}$  ground state with the two strongest 2p-1h components of the  $\frac{1}{2}^-$  state in  $^{17}\text{O}$ .

Compared to a "single-particle estimate" of the transition strength the unique first-forbidden decay to the ground state is inhibited by a factor of about 8. Bertsch and Molinari<sup>26</sup> point out that this inhibition can be traced to the repulsive nature of the  $T = 1$  particle-hole force. The transition can be written schematically as

$$|2p-1h, T = \frac{3}{2}\rangle \xrightarrow{\beta^-} |1p, T = \frac{1}{2}\rangle.$$

Because of the repulsive nature of the  $T = 1$ , p-h

TABLE IV.  $\beta$  decay in the mass-17 system: comparison between theory and experiment and comparison between the  $\beta$  decays of  $^{17}\text{Ne}$  and  $^{17}\text{N}$ .

Transition $J^\pi_f$	$E_f$	$^{17}\text{N}$ decay		$^{17}\text{Ne}$ decay <sup>a</sup>		$\delta = (ft)^+ / (ft)^- - 1$	Theory	
		$E_f$	$f_n t$	$E_f$	$f_n t$		$f_n t$	Source
$\frac{5}{2}^+$	0		$(3.32 \pm 0.98) \times 10^9$	0	$(3.81 \pm 1.15) \times 10^9$	...	$1.44 \times 10^9$	b
$\frac{1}{2}^+$	0.87		$(9.70 \pm 1.68) \times 10^9$	0.50	$(1.42 \pm 0.65) \times 10^9$	...		
$\frac{1}{2}^-$	3.06		$(7.56 \pm 1.12) \times 10^6$	3.11	$(2.78 \pm 0.41) \times 10^6$	$-0.632 \pm 0.077$	$3.12 \times 10^5$	c
$\frac{3}{2}^-$	4.55		$(2.60 \pm 0.11) \times 10^4$	4.61	$(3.91 \pm 0.18) \times 10^4$	$+0.503 \pm 0.094$	$1.00 \times 10^4$	c
$\frac{3}{2}^-$	5.38		$(7.08 \pm 0.25) \times 10^3$	5.48	$(7.19 \pm 0.16) \times 10^3$	$+0.015 \pm 0.042$	$6.31 \times 10^5$	c
$\frac{1}{2}^-$	5.94		$(2.75 \pm 0.29) \times 10^4$	6.04	$(2.61 \pm 0.07) \times 10^4$	$-0.051 \pm 0.103$	$2.0 \times 10^4$	c

<sup>a</sup> Reference 25.

<sup>b</sup> Reference 26.

<sup>c</sup> Reference 27.

force the particle and hole in the  $^{17}\text{N}$  wave function are separated as much as is possible; hence, since the transition matrix element depends on the amplitude of the particle at the hole, inhibition follows. Using a wave function for the  $^{17}\text{N}$  ground state derived using the "bare"  $G$ -matrix interaction of Kuo and Brown, the matrix element quoted by Bertsch and Molinari<sup>26</sup> implies  $f_1 t = 1.44 \times 10^9$  compared with the experimentally determined value of  $(3.32 \pm 0.98) \times 10^9$ . That is, their calculations are qualitatively correct, but they still do not produce enough inhibition.

#### B. Comparison with the Mirror Decays from $^{17}\text{Ne}$

In Table IV we compare the  $f_0 t$  values for four allowed transitions from  $^{17}\text{N}$  and  $^{17}\text{Ne}$  to states in  $^{17}\text{O}$  and  $^{17}\text{F}$ , respectively. The simplest expectation is that  $f_0 t$  values for mirror transitions should be equal. For  $\beta$  decay in even- $A$  systems this has been shown to be so<sup>13</sup> when the small correction is made for the difference in binding energy in the initial state of the proton making the transition in the  $\beta^+$  decay and its mirror neutron in the  $\beta^-$  decay. The absence of any unexplained asymmetry in the mirror  $\beta$  decays in even- $A$  systems can be taken to indicate that at least at the level of a few percent there is no evidence for the existence of a second-class current term in the  $\beta$ -decay Hamiltonian.<sup>31, 13, 28</sup> However, in the odd- $A$  systems (mass 9, 13, 17, and 25) there is evidence<sup>13</sup> from previous experiments for much larger mirror asymmetries in  $\beta$  decay. As will be seen, the present results isolate this asymmetry (for mass 17) in the mirror decays to a pair of levels and thus enable us to give a qualitative explanation of the possible cause of this asymmetry.

The sixth column of Table IV shows the value of  $\delta = (ft)^+ / (ft)^- - 1$ , where  $(ft)^+$  is the  $f_0 t$  value calculated for the positron decay. As mentioned above,  $\delta$  is expected to be close to zero, and indeed, for two of the strongest states this is so. The  $f_0 t$  values for the mirror decays to the second  $\frac{3}{2}^-$  and second  $\frac{1}{2}^-$  states are (within the errors) equal. However, for the first  $\frac{1}{2}^-$  state,  $\delta = -(0.632 \pm 0.077)$  while for the first  $\frac{3}{2}^-$  state,  $\delta = +(0.503 \pm 0.094)$ . If we take into account the fact that the transition

rates to the first  $\frac{1}{2}^-$  state result from the near cancellation of two large matrix elements, the large value of  $\delta$  for this transition is perhaps not surprising. For the first  $\frac{3}{2}^-$  state, however, the transitions are both quite strong and the large value of  $\delta$  is a surprise. From an examination of the data for the even- $A$  systems<sup>13</sup> this large value cannot be explained by the binding-energy differences in the parent nuclei. Nor can it be ascribed to second-class currents.<sup>13</sup> A remaining possibility lies in the fact that seven of the eight levels in the daughter nuclei that we are discussing are unbound.

An examination of the widths of the levels in question reveals that for the lowest  $\frac{3}{2}^-$  state the ratio of the widths  $\Gamma(^{17}\text{F})/\Gamma(^{17}\text{O}) = 5.1$  while for the second  $\frac{3}{2}^-$  and second  $\frac{1}{2}^-$  states the widths are more nearly comparable:  $\Gamma(^{17}\text{F})/\Gamma(^{17}\text{O}) = 1.7$  and  $0.89$ , respectively. The explanation for the large value of  $\delta$  for the lowest  $\frac{3}{2}^-$  states may well lie here. Rather naively we could look at it like this: For the  $^{17}\text{N}$   $\beta$  decay a neutron changes to a proton (the 16 other particles composing the "core" are unaffected) and then a further neutron (one of the "core" particles) is emitted. This neutron in  $^{17}\text{O}$  is nearer to being bound than is the corresponding proton in  $^{17}\text{F}$ , hence the overlap of the bound  $^{17}\text{N}$  "core" with the  $^{17}\text{O}$  core in the  $\beta$  decay will be greater than the overlap of the bound  $^{17}\text{Ne}$  "core" with the  $^{17}\text{F}$  "core." (The wave function of the much less strongly bound proton in  $^{17}\text{F}$  will spread out more than the wave function of the neutron in  $^{17}\text{O}$ .) Qualitatively this gives the correct relative size for the two  $\beta$ -decay matrix elements: For the  $^{17}\text{N} \rightarrow ^{17}\text{O}$  transition which has the lower  $ft$  value, the overlap of the  $^{17}\text{N}$  and  $^{17}\text{O}$  "cores" is greater than the overlap for the corresponding  $^{17}\text{Ne} \rightarrow ^{17}\text{F}$  transition. We will not attempt a more quantitative explanation at this time.

#### ACKNOWLEDGMENTS

We thank Dr. E. K. Warburton who was instrumental in bringing this problem to our attention, Professor D. H. Wilkinson for several useful discussions, and K. W. Jones for help in providing advice, a computer program, and the  $^3\text{He}$  proportional counter.

†Work supported by the Lockheed Independent Research Program.

<sup>1</sup>B. E. F. Macefield, B. Wakefield, and D. H. Wilkinson, Nucl. Phys. **A131**, 250 (1969).

<sup>2</sup>K. W. Jones, W. R. Harris, M. T. McEllistrem, and D. E. Alburger, Phys. Rev. **186**, 978 (1969)

<sup>3</sup>S. Hinds, R. Middleton, A. E. Litherland, and D. J. Pullen, Phys. Rev. Lett. **6**, 113 (1961).

<sup>4</sup>N. Knable, E. O. Lawrence, C. E. Leith, B. J. Moyer, and R. L. Thornton, Phys. Rev. **74**, 1217 (1948).

<sup>5</sup>L. W. Alvarez, Phys. Rev. **75**, 1127 (1949).

<sup>6</sup>N. Bohr and J. A. Wheeler, Phys. Rev. **56**, 426 (1939).

<sup>7</sup>E. Hayward, Phys. Rev. **75**, 917 (1949).

<sup>8</sup>G. J. Perlow, W. J. Ramler, A. F. Stehney, and J. L. Yntema, Phys. Rev. **122**, 899 (1961).

<sup>9</sup>J. Gilat, G. D. O'Kelley, and E. Eichler, Bull. Am.



- Phys. Soc. 8, 320 (1963).
- <sup>10</sup>M. G. Silbert and J. C. Hopkins, Phys. Rev. 134, B16 (1964).
- <sup>11</sup>Earlier work is summarized by F. Ajzenberg-Selove, Nucl. Phys. A166, 1 (1971).
- <sup>12</sup>D. E. Alburger and D. H. Wilkinson, Phys. Rev. C 6, 2019 (1972).
- <sup>13</sup>D. H. Wilkinson, D. R. Goosman, D. E. Alburger, and R. E. Marrs, Phys. Rev. C 6, 1664 (1972); D. H. Wilkinson, Phys. Rev. Lett. 27, 1018 (1971).
- <sup>14</sup>I. S. Towner, E. K. Warburton, and G. T. Garvey, Ann. Phys. (N. Y.) 66, 674 (1971); E. K. Warburton, G. T. Garvey, and I. S. Towner, *ibid.* 57, 174 (1970). See also I. S. Towner and J. C. Hardy, Nucl. Phys. A179, 489 (1972). These latter authors discuss first-forbidden nonunique  $\beta$  transitions in light nuclei.
- <sup>15</sup>B. Margolis and N. de Takaesy, Can. J. Phys. 44, 1431 (1966); Phys. Lett. 15, 329 (1965); M. Hirata, Prog. Theor. Phys. 43, 1526 (1970); P. J. Ellis and T. Engelard, Nucl. Phys. A144, 161 (1970).
- <sup>16</sup>R. E. McDonald, private communication.
- <sup>17</sup>F. Ajzenberg-Selove, Nucl. Phys. A190, 1 (1972).
- <sup>18</sup>P. M. Endt and C. Van der Leun, Nucl. Phys. A105, 1 (1967).
- <sup>19</sup>K. L. Coop and H. A. Grench, LMSC Report No. LMSC 6-67-65-67 (unpublished); private communication.
- <sup>20</sup>C. D. Swartz and G. E. Owen, in *Fast Neutron Physics* edited by J. B. Marion and J. L. Fowler (Interscience, New York, 1960); T. B. Grandy, Ph. D. thesis, University of Alberta, 1967 (unpublished).
- <sup>21</sup>D. L. Smith, R. G. Polk, and T. G. Miller, Nucl. Instrum. Methods 64, 157 (1968); R. Batchelor, W. B. Gilboy, J. B. Parker, and J. H. Towle, *ibid.* 13, 70 (1961).
- <sup>22</sup>R. Batchelor and G. C. Morrison, in *Fast Neutron Physics* (see Ref. 20).
- <sup>23</sup>KFK Report No. KFK 120 (EANDC-E-35U), December 1962 (unpublished), neutron cross sections for fast reactor materials, Pts. II and III.
- <sup>24</sup>R. Batchelor, R. Aves, and T. H. R. Skyrme, Rev. Sci. Instrum. 26, 1037 (1955).
- <sup>25</sup>J. C. Hardy, J. E. Esterl, R. G. Sextro, and J. Cerny, Phys. Rev. C 3, 700 (1971).
- <sup>26</sup>G. Bertsch and A. Molinari, Nucl. Phys. A148, 87 (1970).
- <sup>27</sup>M. Hirata, Prog. Theor. Phys. 43, 1526 (1970).
- <sup>28</sup>E. J. Konopinski, *The Theory of Beta Radioactivity* (Oxford U. P., Oxford, England, 1966).
- <sup>29</sup>J. N. Bahcall, Nucl. Phys. 75, 10 (1966).
- <sup>30</sup>M. Morita, Phys. Rev. 113, 1584 (1959).
- <sup>31</sup>J. N. Huffaker and E. Greuling, Phys. Rev. 132, 738 (1963).